Synthesis and Characterization of Epitaxial FAU-on-EMT Zeolite Overgrowth Materials

Ann M. Goossens,[a] Bart H. Wouters,[a] Piet J. Grobet,[a] Veronique Buschmann,[b] Lucien Fiermans,[c] and Johan A. Martens*[a]

Keywords: Crystal engineering / Epitaxial intergrowth / Overgrowth / Faujasite type Zeolites / Two-step synthesis

Epitaxial FAU zeolite films were achieved on micrometer-sized EMT support crystals using a two-step synthetic procedure, in which EMT support crystals with hexagonal-platelet morphology, were added to a synthesis gel for the crystallization of an FAU phase. Identification of the appropriate synthesis parameters made it possible to suppress homogeneous nucleation and initial breeding, and to promote the secondary nucleation of the FAU crystallites on the surface of the EMT support crystals. The presence of both an FAU and an EMT phase was verified with powder X-ray diffraction (XRD). Scanning electron microscopy (SEM) was used to confirm the formation of a layer of FAU crystallites on the EMT support crystals. The growth of the FAU phase was found to start at the corners and edges of the EMT support. An FAU crystallization front progressed from the edges towards the center of the hexagon until the EMT support crystals became completely covered by an FAU zeolite film with a thickness of ca. 300 nm. The compositional difference between the EMT support and the FAU film was investigated with ^{29}Si magic angle spinning (MAS) nuclear magnetic resonance (NMR) spectroscopy, X-ray photoelectron spectroscopy (XPS) and energy-dispersive analysis of X-rays (nano-EDAX). The continuous nature of the film was confirmed by the absence of intracrystalline mesopores, which was evidenced by nitrogen physisorption.

Introduction

The phase-pure zeolite samples used in a diversity of industrial applications are exceptions in the field of zeolite crystallization. Indeed, the majority of zeolite crystallization conditions used result in the formation of physical mixtures of zeolite phases and intergrowth materials. A pure zeolite phase is obtained only when the synthesis parameters are finely tuned. An overview of the different types of intergrowths relevant to zeolites, building on the classification proposed by Rao and Thomas,[1] is provided in Figure 1. Basically, there are two types of intergrowths. Polytypism can be pictured as a regular stacking, without mismatch of bonds, of different structurally uniform domains in each individual zeolite crystal. Epitaxy involves the oriented overgrowth of a zeolite crystal with a compositionally or structurally different zeolite phase. These epitaxial intergrowths, also called overgrowths, can be isotactic. This means that every atom of the interface belongs to both flanking structures constituting that interface.

Polytypical intergrowths of FAU/EMT,[2,3] ERI/OFF,[4,5] MFI/MEL,[6,7] MAZ/MOR,[8,9] and the ABC 6-membered ring structures[10,11] have been described in literature. In these layered materials, the individual domains are all externally accessible. Epitaxial intergrowths are the preferred type of intergrowths for obtaining a controlled microscopic separation, as well as the organization of catalytic, molecular sieving and/or adsorptive functions. Only a few examples of epitaxy have been given in literature so far. Wise et al.[12,13] observed an OFF/LEV overgrowth. De Vos Burchart et al.[14] reported the structural overgrowth of zeolite X onto zeolite A crystals. This was realized by a one-step synthesis in which the gel composition giving rise to zeolite A gradually changed to favor the crystallization of zeolite X. An analogous overgrowth of zeolite P on zeolite A was discussed by Breck[15] in terms of partial conversion of zeolite A into zeolite P. In the proposed molecular model for the oriented growth of zeolite X onto zeolite A, the binding efficiency, defined as the percentage of tetrahedrally coordinated T-atoms, is only 67%,[14] thus classifying this overgrowth amongst the nonisotactic systems.

It is common practice to add seed crystals of the desired zeolite phase to a synthesis batch to ensure product purity and/or to increase the rate of crystallization. The presence of seeds can result in a more rapid crystal growth on the surface of the seed crystals or can provoke secondary nucleation. Several mechanisms of secondary nucleation are known, such as micro-attrition, fluid shear, needle breeding and initial breeding, all resulting in the formation of a new population of crystals which eventually remain attached to the surface of the seed crystals.[16] In this work, we investigated the possibility of synthesizing epitaxial intergrowths of FAU-on-EMT by a two-step synthetic procedure, similar to seeding, in which a zeolite layer is grown over support crystals by a conventional crystallization method. Structural overgrowths of zeolite X onto zeolite A, and vice-versa,

[a] Centrum voor Oppervlaktechemie en Katalyse, Departement Interfasechemie, K. U. Leuven,
Kardinaal Mercierlaan 92, 3001 Heverlee (Leuven), Belgium
Fax: (internat.) + 32-16/321998
E-mail: johan.martens@agr.kuleuven.ac.be
[b] Strukturforschung, FB Materialwissenschaft, T. U. Darmstadt, Petersenstraße 23, 64287 Darmstadt, Germany
[c] Vakgroep Vaste Stofwetenschappen, Universiteit Gent Krijgslaan 281/S1, 9000 Gent, Belgium

  1434−1948/01/0505−1167 $ 17.50+.50/0

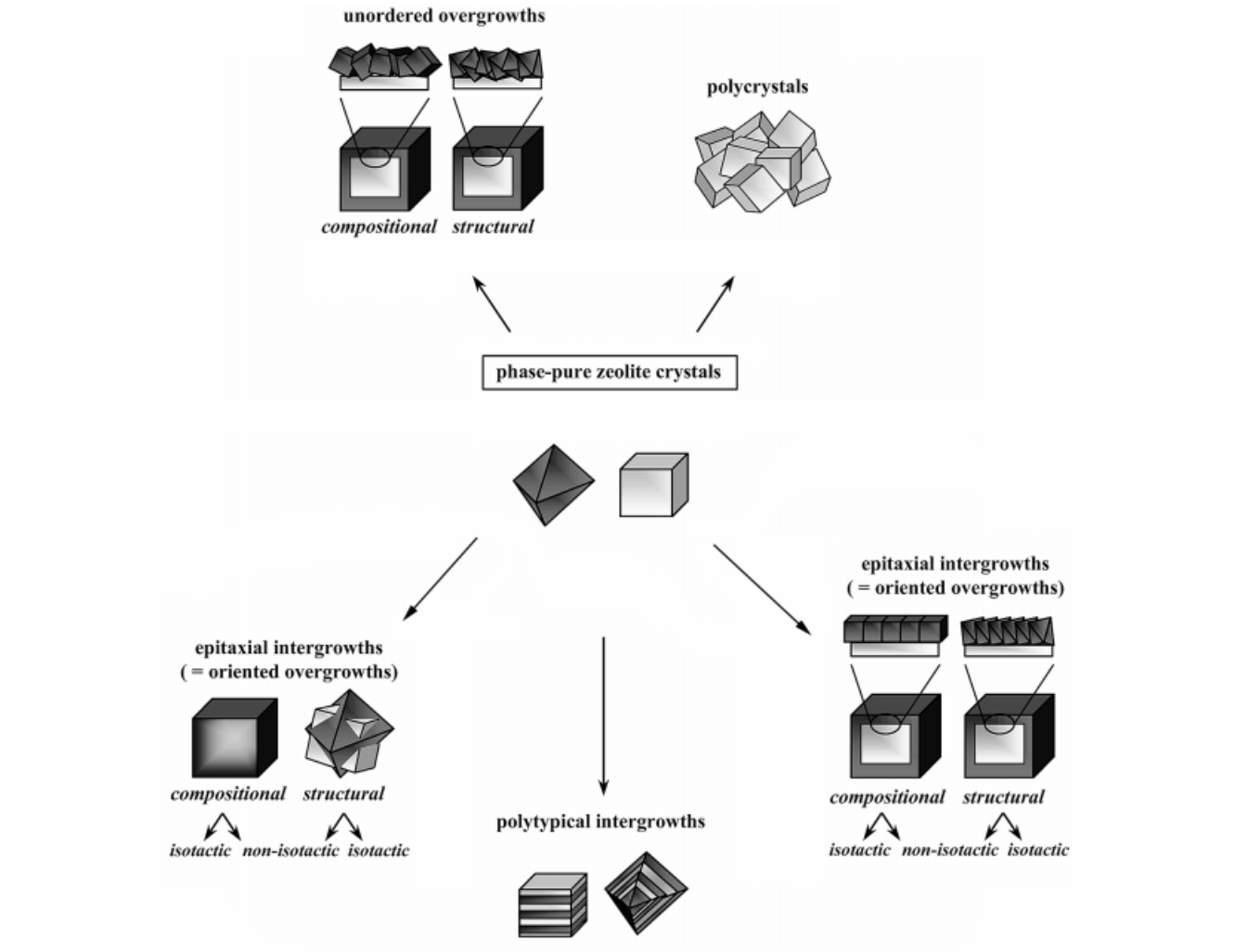

Figure 1. Zeolites and their intergrowths

were previously obtained by using this technique.[14] Compositional overgrowths of ZSM-5 and silicalite were also prepared using such a two-step synthesis.[17–19]

Two structure types with the mnemonic codes FAU and EMT belong to the family of faujasite type zeolites. The FAU and EMT zeolite topologies are structurally related. These zeolite frameworks can be constructed by linking hexagonal prisms into so-called faujasite sheets. Three different relative positions (*a*, *b*, and *c*) exist for these sheets, allowing linkage in the third crystallographic direction. Cubic stacking of faujasite sheets (*abc*) generates the FAU topology, whereas the hexagonal sequence (*ab*) gives rise to the EMT structure. Changes in the stacking sequence from *abc* to *ab* in one crystal produce an FAU/EMT polytypical material. A number of aluminosilicate zeolites have already been identified as polytypical intergrowths of FAU and EMT, ranging from intimately intergrown FAU and EMT layers to segregated FAU and EMT blocks.[3] In previous work, an epitaxial FAU-on-EMT overgrowth material consisting of micrometer-sized hexagonal-platelet EMT support crystals coated with a continuous layer of FAU crystallites was achieved. This was done by introducing the synthesized EMT crystals into a hydrogel for the crystallization of a FAU phase.[20] High-resolution transmission electron microscopy (HRTEM) in combination with selected-area electron diffraction (SAED) revealed the epitaxial relation between the EMT support crystals and the FAU crystallites. The epitaxial relations were: $\{0001\}_{\mathrm{EMTsupport}}$ // $\{111\}_{\mathrm{FAUlayer}}$ and $[11\bar{2}0]_{\mathrm{EMTsupport}}$ // $[\bar{1}10]_{\mathrm{FAUlayer}}$. Furthermore, HREM images of the interface suggested that the overgrowth was isotactic.

The purpose of the present study was to explore the synthesis conditions for the systematic overgrowth of EMT support crystals with an epitaxial and continuous film of FAU crystallites. The synthesis parameters investigated included the molar composition of the synthesis gel, the amount of support crystals added, the pretreatment of the support crystals, the aging and the crystallization time. The

products obtained were identified using X-ray diffraction (XRD) and scanning electron microscopy (SEM). Information about the silicon and aluminum incorporation in the overgrowth materials was obtained from ^{29}Si magic angle spinning (MAS) nuclear magnetic resonance (NMR). The possible presence of compositional heterogeneity in the overgrowing FAU crystallites was investigated using X-ray photoelectron spectroscopy (XPS) and electron nanoprobe analysis of X-rays (nano-EDAX). The crown-ether incorporation was monitored with thermogravimetric-differential thermal analysis (TG-DTA). The continuity of the micropores was verified using nitrogen physisorption.

Results and Discussion

Synthesis of Epitaxial FAU-on-EMT Overgrowth Materials

FAU-on-EMT overgrowth materials were synthesized in two steps. For each experiment, fresh EMT support crystals were prepared using the conventional recipe.[21] According to XRD (Figure 2, a), the EMT support crystals were of excellent crystallinity. The micropore volume of the calcined EMT samples was 0.31 mL/g, confirming the high crystallinity.[21] SEM pictures (Figure 3, a) show the typical hexagonal-platelet morphology. The diagonal dimension of the hexagonal prisms was between 2 and 3 μm, whereas the height varied from 0.5 to 1 μm. The different EMT samples used as supports were not phase-pure, but contained up to 30 wt-% of the FAU structure type. The FAU impurity was detected by XRD as explained in the FAU/EMT quantification section (vide infra). In the SEM pictures, some isolated octahedras were detected next to the abundant hexagonal prisms assigned to the EMT phase. These octahedrally shaped crystals are typical for FAU zeolites. However, their number was too small relative to the amount of FAU estimated by XRD. Most likely, part of the FAU impurity was present as a polytypical intergrowth with EMT. The presence of ca. 10 wt-% of polytypical FAU in EMT samples is not unusual and was also found by other workers.[2,22]

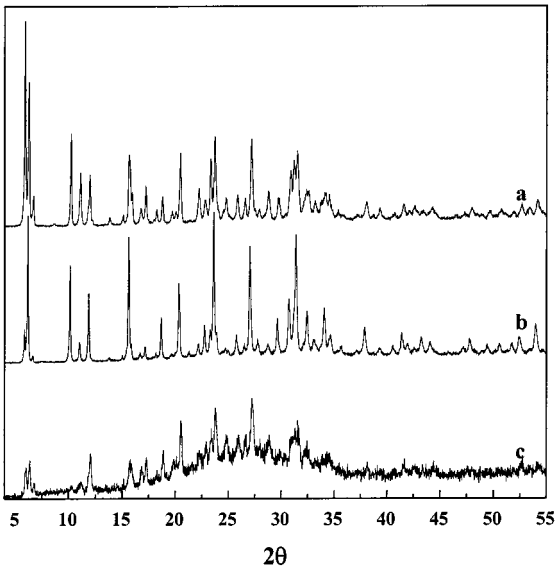

Figure 2. Powder X-ray diffraction patterns of calcined (a) EMT support crystals, (b) sample FauEmt-1a and (c) sample FauEmt-3a

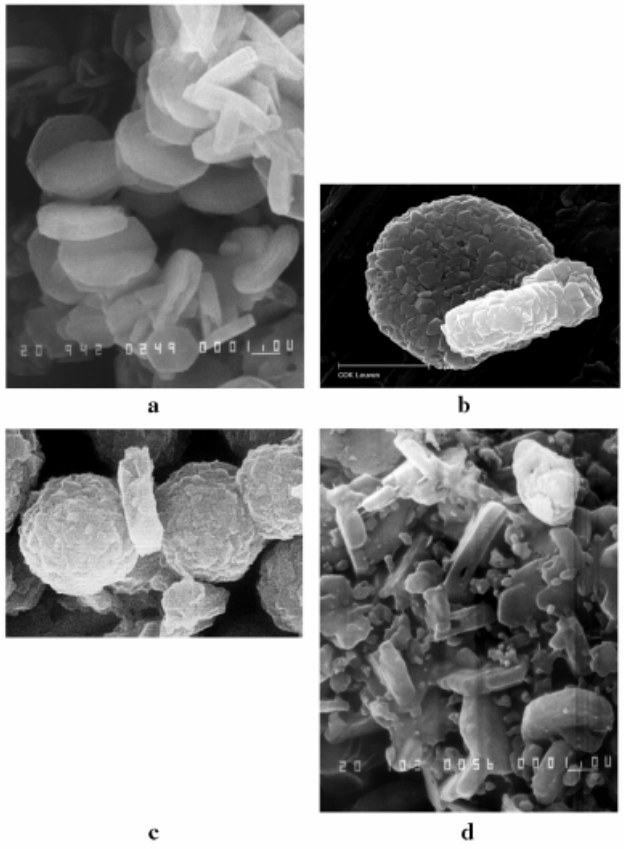

Figure 3. SEM pictures of (a) EMT support crystals, (b, c) sample FauEmt-1a, and (d) sample FauEmt-3a

In the second step, the EMT support crystals were added to a synthesis gel for the crystallization of a FAU phase, which optionally contained crown-ether molecules. Different experiments were conducted in order to explore the influence of the molar composition of the synthesis gel, the amount of EMT support crystals added, the pretreatment of the support crystals, the aging and the crystallization time (Table 1). The products obtained were characterized using powder X-ray diffraction (XRD) and scanning electron microscopy (SEM) (Table 1). The sample notation refers to the crystallographic nature of both phases (Fau for cubic and Emt for hexagonal faujasite). The Arabic number following the hyphen refers to a specific synthesis gel composition, whereas the final letter points to a specific set of synthesis parameters.

Influence of the Molar Composition of the FAU Synthesis Gel

In the first set of experiments (No. 1−5, Table 1), an amount of the synthesized EMT support crystals, typically 0.20 g per g of gel, was added to a freshly prepared FAU synthesis gel which optionally contained crown-ether molecules. The mixtures of gel and support crystals were immediately heated to the crystallization temperature of 373 K. Crystallization took 3 d.

In the literature, several aluminosilicate hydrogel compositions and inorganic bases have been proposed to pro-

Table 1. Molar composition of the FAU synthesis gel, the crystallization conditions and nature of the product obtained

No.	Sample	10 SiO_2; 1 Al_2O_3; x Na_2O; y 15-crown-5; z 18-crown-6; 135 H_2O					g support/g gel		Support pretreatment	t_{293K} + t_{373K}[a] [h]	Product[b]
		x	y	z	Na_2O/SiO_2	OH^-/SiO_2	wet	calcined			
1	FauEmt-1a	3.75	0.00	0.00	0.375	0.75	0.20	0.08	none	0 + 72	FAU-on-EMT
2	FauEmt-2a	3.75	0.00	0.97	0.375	0.75	0.21	0.08	none	0 + 72	FAU-on-EMT
3	FauEmt-3a	2.40	0.97	0.00	0.240	0.48	0.21	0.09	none	0 + 72	EMT + amorphous
4	FauEmt-4a	3.75	0.97	0.00	0.375	0.75	0.20	0.09	none	0 + 72	FAU-on-EMT
5	FauEmt-5a	3.40	0.97	0.00	0.340	0.48	0.21	0.08	none	0 + 72	FAU-on-EMT
6	FauEmt-1b	3.75	0.00	0.00	0.375	0.75	0.41	0.17	none	0 + 72	FAU-on-EMT
7	FauEmt-1c	3.75	0.00	0.00	0.375	0.75	0.59	0.25	none	0 + 72	FAU-on-EMT
8	FauEmt-1d	3.75	0.00	0.00	0.375	0.75	0.10	0.04	none	0 + 72	FAU-on-EMT + FAU
9	FauEmt-2b	3.75	0.00	0.97	0.375	0.75	0.40	0.16	none	0 + 72	FAU-on-EMT
10	FauEmt-2c	3.75	0.00	0.97	0.375	0.75	0.59	0.24	none	0 + 72	FAU-on-EMT
11	FauEmt-2d	3.75	0.00	0.97	0.375	0.75	0.20	0.07	washing	0 + 72	FAU-on-EMT + FAU
12	FauEmt-2e	3.75	0.00	0.97	0.375	0.75	N.D.[c]	0.07	washing, drying and calcining	0 + 72	FAU-on-EMT + FAU
13	FauEmt-2f	3.75	0.00	0.97	0.375	0.75	0.40	0.15	none	0 + 4	EMT + amorphous
14	FauEmt-2g	3.75	0.00	0.97	0.375	0.75	0.40	0.15	none	0 + 8	EMT + amorphous
15	FauEmt-2h	3.75	0.00	0.97	0.375	0.75	0.40	0.15	none	0 + 12	EMT + amorphous
16	FauEmt-2i	3.75	0.00	0.97	0.375	0.75	0.40	0.15	none	0 + 16	EMT + amorphous
17	FauEmt-2j	3.75	0.00	0.97	0.375	0.75	0.40	0.15	none	0 + 20	FAU-on-EMT + amorphous
18	FauEmt-2k	3.75	0.00	0.97	0.375	0.75	0.40	0.15	none	0 + 24	FAU-on-EMT
19	FauEmt-2l	3.75	0.00	0.97	0.375	0.75	0.40	0.15	none	0 + 48	FAU-on-EMT
20	FauEmt-2m	3.75	0.00	0.97	0.375	0.75	0.40	0.15	none	0 + 72	FAU-on-EMT
21	FauEmt-2n	3.75	0.00	0.97	0.375	0.75	0.40	0.15	none	0 + 96	FAU-on-EMT
22	FauEmt-2o	3.75	0.00	0.97	0.375	0.75	0.40	0.15	none	0 + 120	FAU-on-EMT
23	FauEmt-3b	2.40	0.97	0.00	0.240	0.48	0.21	0.09	none	0 + 144	EMT + amorphous
24	FauEmt-3c	2.40	0.97	0.00	0.240	0.48	0.24	0.09	none	3 + 72	FAU-on-EMT + FAU

[a] t_{293K} = aging time; t_{373K} = crystallization time. – [b] According to XRD and SEM. – [c] N.D. = not determined.

duce FAU phases under hydrothermal conditions.[15] It is recognized that the alkalinity of the hydrogel, expressed as the OH^-/SiO_2 ratio, is a crucial parameter. Low alkalinities substantially decrease the nucleation, as well as the crystallization rate, yielding poorly crystalline FAU materials. A very alkaline inorganic gel with a Na_2O/SiO_2 ratio of 0.375 was used in experiment No. 1 (sample FauEmt-1a, Table 1). According to XRD (Figure 2, b), the product contained a considerable amount of FAU, as well as EMT. Since the diffraction lines of the cubic FAU phase coincide with the lines of the hexagonal EMT phase, the detection of FAU was based on the relative intensities of lines belonging to the hexagonal phase alone and of common reflections of the cubic and the hexagonal phase. SEM pictures (Figure 3, b) revealed that a layer consisting of small crystals, some of which had an octahedral shape, covered all faces of the hexagonal platelets. This morphology indicates that the FAU zeolite has nucleated and grown on all faces of the original hexagonal-platelet EMT support crystals, thus yielding a polycrystalline film. As the support crystals were no longer visible, the FAU film was considered to be continuous. The morphology of the overgrowth material further suggests that all FAU crystallites are oriented with one of their {111} planes parallel to the {0001} planes of the EMT support, classifying this FAU-on-EMT overgrowth material as an epitaxial intergrowth. Besides the EMT support crystals being coated with an oriented layer of FAU crystallites, a small number of roughly spherical particles with irregular surfaces were also observed (Figure 3, c). This particular EMT support originally contained 19 wt-% of FAU, part of it being present as isolated FAU crystals with octahedral morphology. Octahedral particles were no longer present in the overgrowth sample, indicating that the octahedral FAU crystals also became overgrown by a layer of FAU crystallites, resulting in these roughly spherical particles. The absence of octahedral crystals also indicated that homogeneous nucleation and initial breeding, both yielding an undesirable population of isolated FAU crystals, were suppressed.

The EMT-type zeolite can be synthesized from aluminosilicate hydrogels doped with 18-crown-6 ether and characterized by an Na_2O/SiO_2 ratio of 0.24.[23] An FAU phase can be obtained from a similar gel provided the sodium content is increased.[21] Inoculation of an 18-crown-6 ether containing FAU synthesis gel characterized by a high Na_2O/SiO_2 ratio of 0.375 with EMT support crystals (sample FauEmt-2a, Table 1), resulted in the formation of an epitaxial FAU-on-EMT overgrowth material.[20]

According to the original synthesis recipe of Delprato et al.,[23] the FAU structure type can crystallize from an aluminosilicate hydrogel containing 15-crown-5-ether, with an Na_2O/SiO_2 ratio of 0.24. The XRD pattern of the crystallization product obtained from such a gel inoculated with the synthesized EMT support crystals (sample FauEmt-3a, Table 1) is characterized by the presence of a broad amorphous background with maximum intensity around a 2θ value of 25° (Figure 2, c). The sharp diffraction lines correspond to those of the EMT support crystals added. SEM pictures (Figure 3, d) show intact support crystals embedded in an amorphous gel matrix. It is concluded that the overgrowth process did not take place in this system. An attempt was made to favor the overgrowth formation by increasing the Na_2O/SiO_2 ratio of the FAU synthesis gel from 0.24 to 0.375 (sample FauEmt-4a, Table 1). The crys-

tallization of FAU during the second step of the synthetic procedure was confirmed by XRD and SEM. Morphologically, sample FauEmt-4a was similar to sample FauEmt-1a and consisted of hexagonal-platelet EMT support crystals coated with a continuous layer of FAU crystallites. However, by increasing the amount of NaOH in the gel, both the sodium content, as well as the alkalinity were increased. In order to find out whether overgrowth formation was dependent on the sodium content or on the alkalinity, another experiment (No. 5) was performed in which the Na^+ content was increased at a constant OH^-/SiO_2 ratio (sample FauEmt-5a, Table 1). This was done by introducing part of the sodium as sodium aluminate. The product crystallized from such a gel was a FAU-on-EMT overgrowth material, similar to sample FauEmt-4a. Therefore, it is concluded that the sodium content of the gel, rather than the alkalinity, is the crucial parameter.

From experiments No. 1−5 (Table 1), it can be concluded that the synthesized EMT support crystals can be overgrown by a continuous, epitaxial layer of FAU crystallites using sodium aluminosilicate hydrogels, which optionally contained crown-ether molecules, provided the Na_2O/SiO_2 ratio of the gel is higher than or equal to 3.40. The crown-ether seemed to have no influence on the overgrowth morphology.

Influence of the Amount of Support Crystals Added

In the next set of experiments (No. 6−10, Table 1) different amounts of EMT support crystals were added in order to obtain samples with different degrees of overgrowth formation. The weight ratio of gel to support crystals was varied between 1.7:1 and 10:1, while keeping the other synthesis parameters constant, i.e. no aging of the synthesis gel and a crystallization time of 3 d.

The use of different amounts of support crystals allowed us to observe discrete stages in the process of overgrowth formation. Figure 4 (a−d) shows SEM pictures of samples for which decreasing quantities of EMT support crystals were used and illustrate the progress of the overgrowth formation. These pictures suggest that the secondary nucleation preference of the FAU phase decreases in the order, corners = edges > faces. This preference for corners and edges, representing the largest concentration of anchoring points, is observed both in the presence (sample FauEmt-2c, Figure 4, a), as well as in the absence of 18-crown-6 ether molecules (sample FauEmt-1c). At intermediate gel/support ratios, it can be seen that a rim of FAU crystallites progresses towards the center of the hexagonal faces (samples FauEmt-1b, Figure 4, b, and FauEmt-2b). When the weight ratio of the synthesized support crystals per gram of FAU synthesis gel is about 0.20, the EMT support crystals become completely covered with FAU crystallites. All of the FAU crystallites were oriented in the same way with respect to the support (samples FauEmt-2a, Figure 4, c, and FauEmt-1a). Further reduction of the amount of EMT support crystals (sample FauEmt-1d, Figure 4, d) resulted in the formation of roughly spherical FAU(18) crystals with an irregular surface, in addition to completely covering the hexagonal prisms. This indicates that, in this instance, the surface offered by the EMT support crystals is not large enough to suppress homogeneous nucleation from the FAU synthesis gel.

Influence of the Pretreatment of the Support Crystals

Thompson and co-workers[24,25] reported that handling seed crystals (washing, drying or calcining) prior to their addition to a synthesis gel always results in so-called initial breeding, hence yielding a new population of isolated crystals. The degree to which initial breeding occurs is dependent on the manner in which the seed crystals are pretreated. Since the two-step synthetic procedure, applied in this work, to produce overgrowth materials is similar to seeding, pretreatment of the support crystals was expected to be detrimental for the process of overgrowth formation.

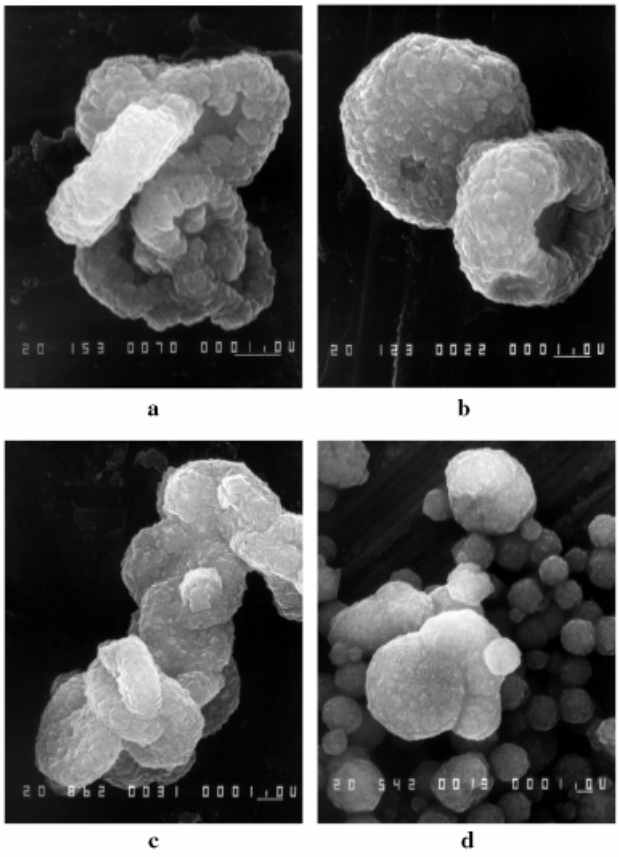

Figure 4. SEM pictures of samples (a) FauEmt-2c, (b) FauEmt-1b, (c) FauEmt-2a, and (d) FauEmt-1d

Two experiments (No. 11 and 12, Table 1) were conducted in which the EMT support crystals were first washed with deionized water until the pH value of the wash water reached 9 (sample FauEmt-2d, Table 1) or washed, dried, and calcined (sample FauEmt-2e, Table 1) before they were added to an FAU gel containing sodium and 18-crown-6 ether. In both cases, there was partial overgrowth with FAU crystallites (Figure 5, a−b). However, overgrowth formation was much less pronounced than in experiments without pretreatment of the support but with the same gel/support

ratio (sample FauEmt-2a, Figure 4, c). An undesirable population of isolated, roughly spherical FAU crystals with diameters of 1 to 2 μm, exhibiting irregular surfaces was also observed. This was most pronounced for sample FauEmt-2e (Figure 5, b). The initial breeding mechanism, favored by the drying and calcination, could have been responsible for the formation of these isolated FAU crystals.

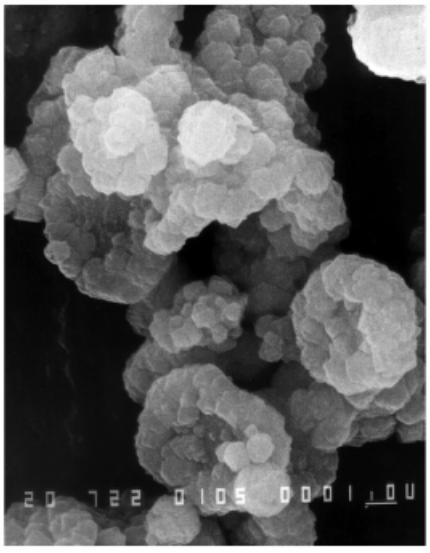

a

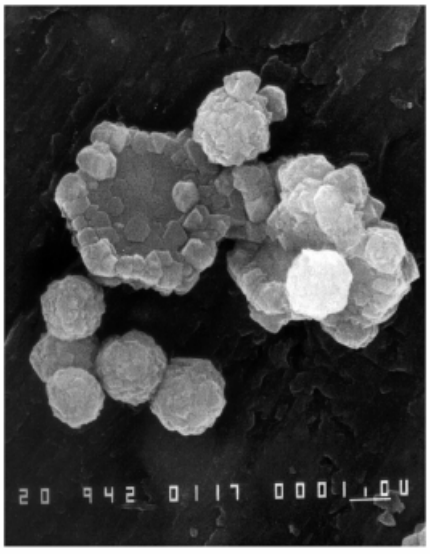

b

Figure 5. SEM pictures of samples (a) FauEmt-2d and (b) FauEmt-2e

Influence of the Aging and Crystallization Time

In all previous experiments the crystallization time was kept constant at 3 d. This length of time was long enough to obtain overgrowth materials from hydrogels with an Na_2O/SiO_2 ratio of 0.34 or 0.375. On the other hand, no crystallization took place from hydrogels with a reduced sodium content. Therefore, a new set of experiments (No. 13−24, Table 1) was conducted in order to investigate the influence of the aging and the crystallization time on the overgrowth process.

Ten overgrowth experiments (No. 13−22, Table 1), in which the synthesized EMT support crystals were added to an FAU synthesis gel containing sodium and 18-crown-6 ether, were performed using crystallization times from 4−120 h (samples FauEmt-2f to FauEmt-2o, Table 1). In the first 16 h of crystallization (samples FauEmt-2f to FauEmt-2i, Table 1), no FAU phase could be observed with XRD (Figure 6, a; sample FauEmt-2i). SEM pictures (Figure 7, a) show EMT support crystals embedded in an amorphous gel matrix. After 20 h of crystallization (sample FauEmt-2j, Table 1), some EMT support crystals were decorated at their edges with small FAU crystallites. A residual amorphous phase was also observed (Figure 7, b). Four hours later (sample FauEmt-2k, Table 1), the amorphous material was no longer present and all EMT support crystals were partially coated with small FAU crystallites (Figure 6, b and Figure 7, c). The use of longer crystallization times did not alter the morphology of the overgrowth product. In this series of experiments (No. 13−22, Table 1), it was clearly shown that the growth of the FAU phase starts at the corners and edges of the hexagonal-platelet EMT support crystals. An FAU crystallization front progresses subsequently from the edges towards the center of the hexagon. The same sequence was encountered in the set of experiments in which the amount of support crystals added was varied, while the crystallization time was kept constant (No. 6−10, Figure 4, a−d).

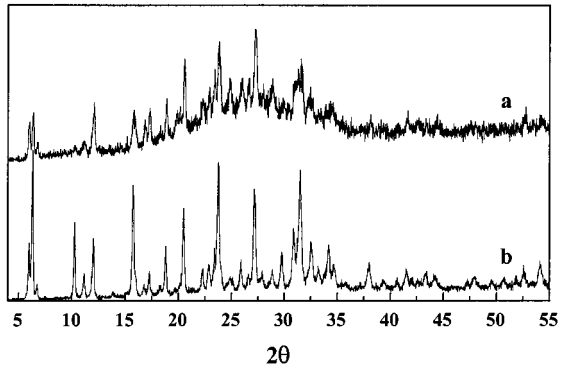

Figure 6. Powder X-ray diffraction patterns of calcined samples (a) FauEmt-2i and (b) FauEmt-2k

In order to evaluate whether a longer crystallization time would be necessary for overgrowth formation in the systems of the present study with a low sodium content, the crystallization time of experiment FauEmt-3a (Table 1) was prolonged from 3 to 6 d (sample FauEmt-3b, Table 1). This did not result in the transformation of the amorphous synthesis gel into a crystalline product, thereby indicating that crystallization of an FAU phase in the presence of support crystals is not possible from freshly prepared synthesis gels characterized by an Na_2O/SiO_2 ratio of 0.24.

Aging the low alkaline FAU synthesis gel containing 15-crown-5 ether for 3 d at room temperature before the EMT support crystals were added to it (sample FauEmt-3c,

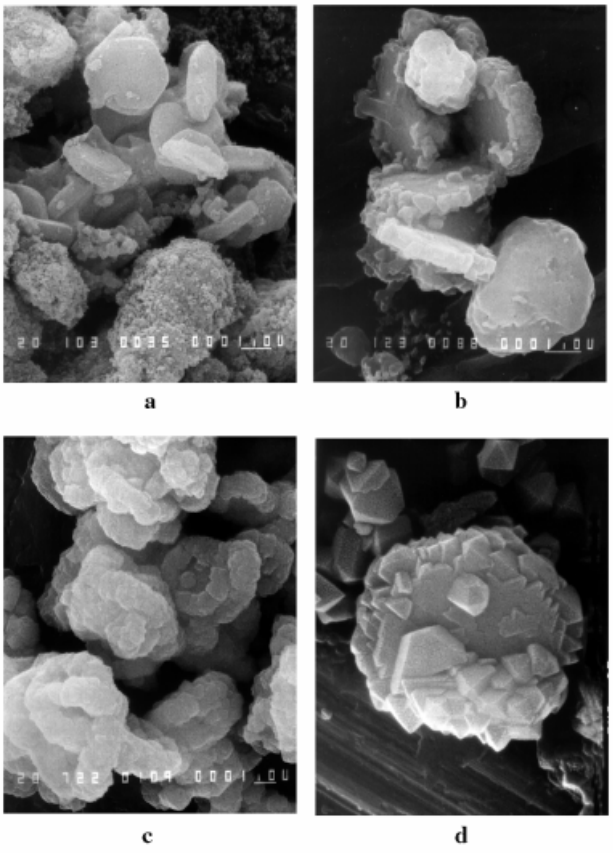

Figure 7. SEM pictures of samples (a) FauEmt-2i, (b) FauEmt-2j, (c) FauEmt-2k, and (d) FauEmt-3c

Table 1), resulted in the formation of an epitaxial FAU-on-EMT overgrowth material. However, the EMT support crystals were not completely covered by FAU crystallites, and a new population of isolated FAU crystals with octahedral morphology was also obtained (Figure 7, d). In this case, the hydrogel was supersaturated, giving rise to homogeneous nucleation of an FAU phase along with secondary nucleation of FAU crystallites on the surface of the EMT support crystals.

FAU/EMT Quantification

The amount of FAU and EMT in the FAU-on-EMT overgrowth materials was estimated with XRD by using a calibration curve. For this purpose, two calcined overgrowth samples were quantified using the Rietveld refinement technique.[26] These reference samples, FauEmt-2a and FauEmt-2c, contained 80 and 51 wt-% of the FAU phase, respectively (Table 2). Most of the FAU-on-EMT overgrowth materials obtained in this study have FAU contents in this range. The reference zeolite powders were physically mixed in five different proportions and the XRD patterns of these mixtures were recorded. The peak intensities of four selected diffraction lines belonging to the EMT phase alone (Table 3) and of five common reflections of the FAU and the EMT phase (Table 3), were obtained by integration and summation. The EMT content (in wt-%) was correlated to the intensity ratio of these sums ($I_{EMT}/I_{EMT+FAU}$). The experimental data points were fitted with the parabolic relation given in Equation (1).

$$\text{EMT (wt-\%)} = 68 \times (I_{EMT}/I_{EMT+FAU})^2 + 108 \times I_{EMT}/I_{EMT+FAU} + 1 \quad (1)$$

The FAU and EMT contents of some selected overgrowth samples and of the EMT support crystals were derived from XRD using Equation (1), and reported as absolute weights in Table 2. It is clear from this table that the weight of EMT in the overgrowth product was systematically lower than the weight of the EMT phase in the support crystals added. This suggests that part of the EMT phase dissolved during the overgrowth process. The dissolution behavior of the EMT crystals was therefore studied in more detail.

Dissolution of the Support Crystals

It is known that in strong mineral bases, siliceous frameworks are more soluble than aluminosilicate frameworks. The reason for this is the more facile base-catalyzed hydrolysis of silyloxy bridges, whereas the tetrahedral aluminum centers in an aluminosilicate lattice are relatively inert to hydroxide attack due to the negative framework charge associated with these centers.[27−29]

In order to obtain some information about the dissolution behavior of the EMT support crystals in basic environments, such as in the gels used for the formation of FAU-on-EMT overgrowth materials, two experiments were conducted. In the first experiment (EMT-A), a FAU synthesis gel containing sodium and 18-crown-6 ether was aged for 3 d at room temperature. The solid phase was separated from the liquid phase by ultra-centrifugation at 17 000 rpm for 2 h. A mass of 5 g of the synthesized EMT crystals was added to 25 mL of this liquid. This particular batch of EMT crystals did not contain any FAU, according to XRD. In the EMT-B experiment, 5 g of the same EMT crystals was suspended in 25 mL of a 2.5 M NaOH solution. The resulting slurries were transferred into PTFE-lined stainless-steel autoclaves, which were kept at 373 K for 3 d. The products were recovered by vacuum filtration, washed with deionized water and dried at 333 K. Calcination was done in a muffle furnace at 823 K for 20 h.

By comparing the weight of the product with that of the EMT crystals added (on a calcined basis), it was found that 52 and 68 wt-% of EMT had dissolved in experiments A and B, respectively. The XRD pattern of EMT-A (Figure 8, a) corresponded to that of EMT. The diffraction lines belonging to the EMT structure type were somewhat less intense than in the original EMT sample (Figure 2, a). In sample EMT-B, XRD confirmed the formation of zeolite P, as well as residual EMT (Figure 8, b). The formation of zeolite P is often observed in Ostwald successive phase transformations of faujasite type zeolites which are left in their mother liquor for some time.[30,31]

The EMT-A and EMT-B samples were examined using SEM (Figure 9, a−b) and HRTEM (Figure 10, a−c). All EMT-A crystals showed dissolution to a similar extent. The dissolution caused the formation of pits over the entire sur-

Table 2. FAU/EMT quantification

Sample	Support EMT [g]	Support FAU[a] [g]	Product EMT [g]	Product FAU [g]	EMT dissolved [g]	FAU dissolved[b] [g]	Support dissolved (%)	Gel [g]	Yield FAU layer [g/g gel]	Support dissolved [g/g gel]
FauEmt-1a	1.93	0.45	1.47	4.20	0.46	0.11	24	28.81	0.13	0.02
FauEmt-2a	1.99	0.44	1.08[c]	4.33[c]	0.91	0.20	46	29.15	0.14	0.04
FauEmt-4ab	2.73	0.00	1.45	4.61	1.28	0.00	47	32.91	0.14	0.04
FauEmt-1b	3.58	0.84	2.83	4.43	0.75	0.18	21	30.82	0.12	0.03
FauEmt-1c	4.66	1.09	4.28	3.50	0.38	0.09	8	23.23	0.11	0.02
FauEmt-2b	3.27	0.72	2.25	3.66	1.02	0.22	31	24.84	0.13	0.05
FauEmt-2c	4.41	0.97	3.11[c]	3.23[c]	1.30	0.29	29	22.41	0.11	0.07
FauEmt-2k	3.50	1.23	3.25	4.68	0.25	0.09	7	32.14	0.11	0.01
FauEmt-2l	2.81	0.99	2.58	3.71	0.23	0.08	8	25.80	0.11	0.01
FauEmt-2m	2.70	0.95	2.51	3.61	0.19	0.07	7	24.82	0.11	0.01
FauEmt-2n	2.73	0.96	2.41	3.62	0.32	0.11	12	25.09	0.11	0.02
FauEmt-2o	2.71	0.95	2.19	3.73	0.52	0.18	19	24.82	0.12	0.03

[a] FAU impurity content of the EMT support samples. – [b] Assuming that the FAU impurity dissolved in the same proportion as the EMT phase. – [c] According to Rietveld refinement.

Table 3. Diffraction angles of the XRD lines used to estimate the amount of FAU and EMT in the FAU-on-EMT overgrowth samples

2θ [°]	Phase	2θ [°]	Phase	2θ [°]	Phase
10.1	FAU+EMT	15.6	FAU+EMT	25.7	FAU+EMT
11.0	EMT	17.2	EMT	28.7	EMT
11.9	FAU+EMT	22.2	EMT	29.5	FAU+EMT

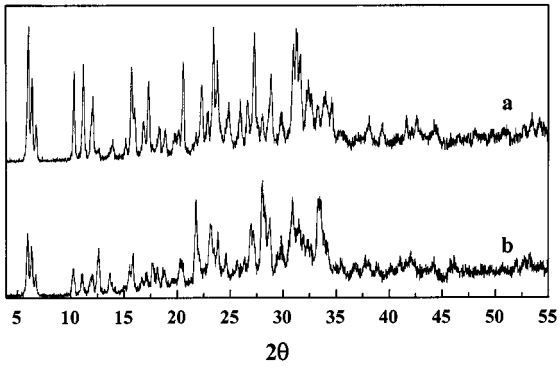

Figure 8. Powder X-ray diffraction patterns of calcined samples (a) EMT-A and (b) EMT-B

face of the crystals (Figure 9, a, and Figure 10, a). The higher degree of dissolution of sample EMT-B relative to that of EMT-A was seen in the SEM and HRTEM pictures (Figure 9, b, and Figure 10, b–c). Many EMT-B crystals had decomposed into smaller fragments. Some particles retained their initial hexagonal-platelet morphology and were more strongly dissolved at the center than at the outer rim. The larger particles with smooth surfaces, which could be observed in sample EMT-B with the SEM (Figure 10, b), are most likely zeolite P crystals. It is known from the literature that the Si and Al positioning in the EMT crystals synthesized with 18-crown-6 ether is not uniform.[32] The 12-MRs circumscribing the hyperchannels running in the direction perpendicular to the hexagonal faces are more siliceous (Si/Al ratio of 5.7) than the 12-MRs delineating the channels running parallel to the hexagonal faces and connecting the hypocages with the hyperchannels. This could explain why the dissolution was more pronounced in the direction of the hyperchannels and why the outer rim, exposing more Al-rich 12-MRs, is more resistant to dissolution by the base.

The Si/Al ratios of the partially dissolved EMT crystals of samples EMT-A and EMT-B, as determined with nano-EDAX, varied between 2.2 and 1.3, depending on the degree of dissolution. These low values indicate that EMT samples recovered after base-treatment are significantly enriched with aluminum, confirming the selective removal of SiO_2 in the alkaline solutions. Phase-pure EMT crystals with such low Si/Al ratios have not been reported previously. The low Si/Al ratios imply that silicon has been substituted by aluminum in the residual EMT framework. Reinsertion of aluminum into faujasite type zeolites is possible provided a concentrated solution of a strong base is present.[33]

The parent EMT sample, and the EMT-A and EMT-B samples were characterized with nitrogen physisorption. The external surface area, the micropore volume and the micropore diameter calculated from the adsorption branch of the isotherms are given in Table 4. All isotherms are of type I revealing the presence of a microporous solid. The micropore volumes of EMT-A and EMT-B were 0.26 and 0.14 mL/g (Table 4), respectively. In both samples, there was very little nitrogen uptake in the P/P_0 range of 0.1 to 0.8, indicating the absence of capillary condensation in small mesopores. The nitrogen uptake at P/P_0 values exceeding 0.8 is indicative of the presence of large mesopores, typically present in the interstitial voids between particles. The generation of 28 and 37 m^2/g of external surface area in EMT-A and EMT-B, respectively, compared with 4 m^2/g in the original EMT sample, can be explained by an increase of the surface roughness (sample EMT-A) and a decrease in the particle size (sample EMT-B). It is concluded that the dissolution process did not generate mesopores in the crystals, suggesting that the dissolution occurred through the removal of framework fragments in a block-wise manner. The micropore diameter determined using the Horvath–Kawazoe approach increased from 0.64 to

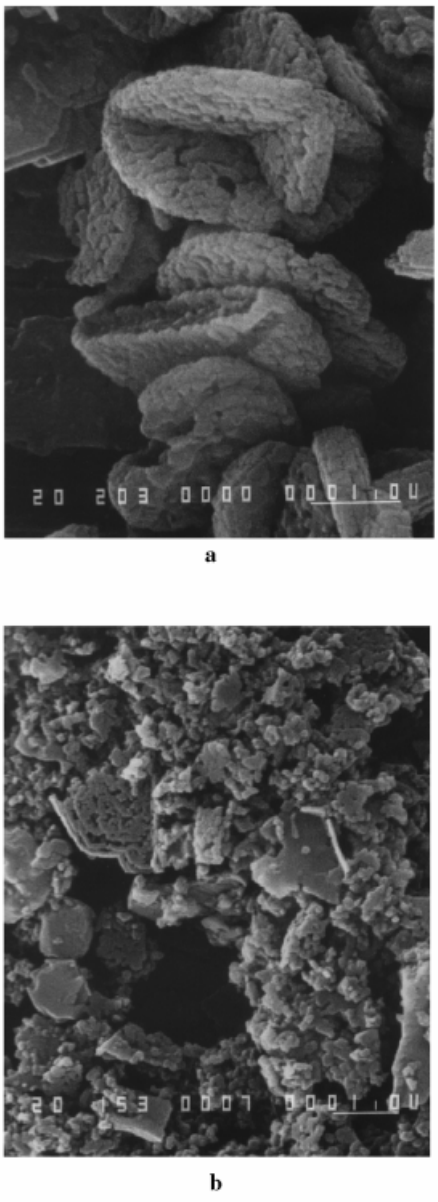

Figure 9. SEM pictures of samples (a) EMT-A and (b) EMT-B

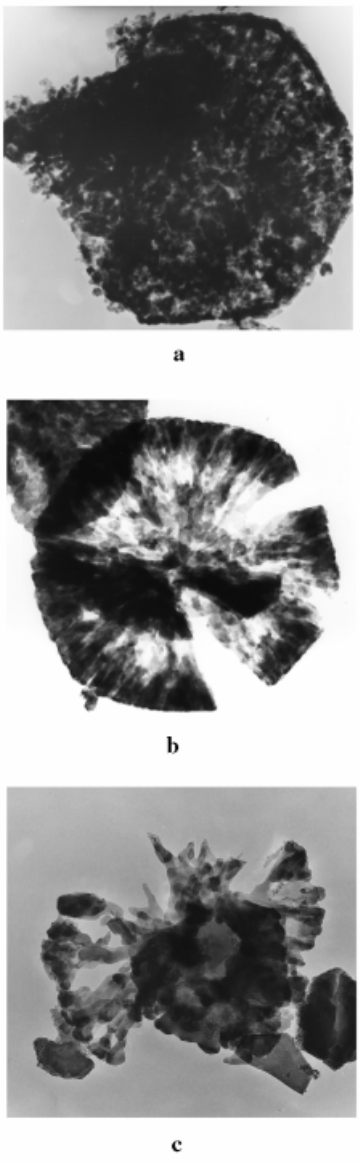

Figure 10. HRTEM pictures of samples (a) EMT-A and (b, c) EMT-B

0.65 nm for sample EMT-A. Such an increase is in agreement with the enrichment of the framework with aluminum.

Characterization of Both the FAU and the EMT Phase

In the previous section, it was shown how EMT crystals partially dissolve in the alkaline conditions of synthesis gels. In the two-step synthetic procedure for overgrowth formation, the material balance suggested that a significant part of the EMT crystals dissolved (Table 2). In this section, the FAU-on-EMT overgrowth materials were characterized in more detail in order to find out the extent to which the EMT support crystals were altered during the overgrowth process.

FAU-on-EMT overgrowth samples synthesized with three types of FAU gels and with different degrees of overgrowth formation were characterized using nitrogen physisorption (Table 5). The adsorption isotherms of the FAU-on-EMT overgrowth materials were similar to those of the EMT support crystals. The absence of nitrogen uptake in the P/P_0 range of 0.1 to 0.8 was indicative of the absence of mesopores inside the particles, and thus for the continuous nature of the FAU film. The micropore volume of all samples was between 0.29 and 0.32 mL/g (Table 5), as is expected for FAU and EMT phases of high quality.[21] The high micropore volume also indicated that the micropores of both the FAU layer, as well as the EMT support were accessible to nitrogen. For all overgrowth samples investigated, the specific external surface area was below 10 m^2/g (Table 5), this value being only a little higher than the specific external surface area of the support crystals (4 m^2/g). The external surface area increased proportionally with the

Table 4. External surface area, micropore volume and micropore diameter of calcined EMT samples, before and after base-treatment, as determined from their N_2 adsorption isotherms

Sample	External surface area [m^2/g]	Micropore volume [mL/g]	Micropore diameter [nm]
EMT	4	0.31	0.64
EMT-A	28	0.26	0.65
EMT-B	37	0.14	–[a]

[a] Determination not reliable.

Table 5. External surface area, micropore volume and micropore diameter of selected overgrowth samples (calcined), as determined from their N_2 adsorption isotherms

Sample	FAU (wt-%)	External surface area [m^2/g]	Micropore volume [mL/g]	Micropore diameter [nm]
FauEmt-1a	74	9	0.29	0.67
FauEmt-2a	80	8	0.30	0.68
FauEmt-4a	76	9	0.29	0.65
FauEmt-1b	61	7	0.29	0.66
FauEmt-1c	45	5	0.30	0.65
FauEmt-2b	51	4	0.32	0.65
FauEmt-2c	62	7	0.31	0.67

FAU content of the overgrowth samples (Table 5). Therefore, the specific external surface area could be attributed to the FAU crystallites exposing more external surface area than the EMT support crystals, owing to their smaller size. The micropore diameters derived from the nitrogen adsorption isotherms using the Horvath–Kawazoe approach were in the range of 0.65 to 0.68 nm, and in agreement with the presence of 12-MRs. The micropore diameters showed a systematic increase with increasing FAU content (Table 5). Nitrogen physisorption showed that the EMT core of the FAU-on-EMT overgrowth materials was rather intact. Furthermore, it showed that the significant alterations, observed in the base-treated EMT-A and EMT-B samples, did not take place in the EMT crystals, which were overgrown by a layer of FAU crystallites. It seems that of all the EMT support crystals added, a fraction became overgrown, whereas the rest dissolved completely. The absence of particles resembling the partially dissolved EMT-A and EMT-B samples in the SEM images of all FAU-on-EMT overgrowth materials supports this hypothesis.

The distribution of Si(*n*Al) environments in the EMT support crystals and in some selected FAU-on-EMT overgrowth samples was determined with ^{29}Si MAS NMR. The ^{29}Si MAS NMR spectrum of the EMT support crystals is shown in Figure 11, a. This spectrum can be simulated by five Gaussian peaks with the maxima positioned at chemical shift values of $\delta = -105.80$, assigned to Si(0Al); at $\delta = -101.21$ and -99.69, both assigned to Si(1Al); at $\delta = -94.06$, assigned to Si(2Al); and at $\delta = -89.13$, assigned to Si(3Al). A signal for Si(4Al) environments expected at $\delta \approx -84$ could not be distinguished from the background. From this simulation, the framework Si/Al ratio of the support crystals was calculated to be 3.4. The ^{29}Si MAS NMR spectra of FAU-on-EMT overgrowth samples with FAU content between 74 and 80 wt-%, and prepared using three types of FAU synthesis gels (samples FauEmt-1a, FauEmt-2a, and FauEmt-4a) are shown in Figure 11 (b–d). The spectra were simulated with Gaussian curves, as explained for the support crystals. An additional small line at $\delta = -84$, representing Si(4Al) environments, was present. The Si(*n*Al) distributions and the framework Si/Al ratios of the support crystals and the overgrowth samples are presented in Table 6. The Si(*n*Al) distributions are similar amongst the selected overgrowth materials, but significantly different from that of the support crystals. The population of silicon in the Si(0Al) and Si(1Al) sites is lower, and that in the Si(2Al) and Si(3Al) sites is higher than in the support (Table 6). The framework Si/Al ratio of the overgrowth sample prepared from an inorganic aluminosilicate hydrogel was 2.7 (sample FauEmt-1a, Table 6). In the presence of crown-ether molecules, a slightly higher Si/Al ratio of 2.9 was obtained (samples FauEmt-2a and FauEmt-4a, Table 6).

In another series of samples, the degree of overgrowth formation was varied between 51 and 80 wt-% by decreasing the amount of support crystals added to an FAU synthesis gel containing sodium and 18-crown-6 ether (samples FauEmt-2c to FauEmt-2a). The Si(*n*Al) distributions of these overgrowth samples are also given in Table 6. It was observed that when the FAU content increased, the concentration of Si(4Al), Si(3Al), and Si(2Al) environments increased, whereas the population of silicon in the Si(1Al) and the Si(0Al) sites decreased. This resulted in a decreasing framework Si/Al ratio with increasing FAU content from 3.1 for an FAU content of 51 wt-% to 2.9 for an FAU content of 80 wt-% (Table 6). The increase in the micropore diameter with increasing FAU content of the FAU-on-EMT overgrowth materials (Table 5) can be explained by the en-

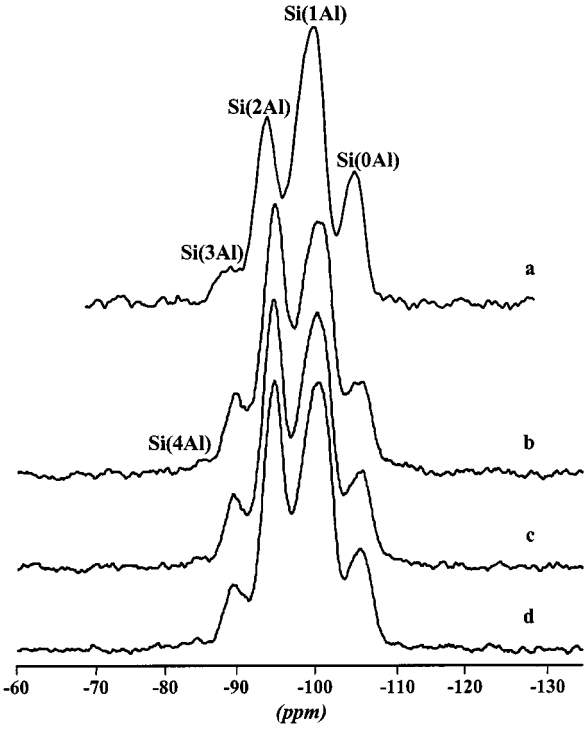

Figure 11. ^{29}Si MAS NMR spectra of: (a) calcined EMT support crystals, and calcined overgrowth samples (b) FauEmt-1a, (c) FauEmt-2a, and (d) FauEmt-4a

represent the weight fractions of support and FAU layer in the FAU-on-EMT overgrowth products, respectively.

$$Si/Al_{FAUlayer} = [Si/Al_{overgrowth} - Si/Al_{support} \times fraction_{support}]/fraction_{FAUlayer} \quad (2)$$

The $Si/Al_{FAUlayer}$ ratios of samples prepared using different FAU gel compositions (samples FauEmt-1a, FauEmt-2a and FauEmt-4a) are listed in Table 6. The FAU layer grown in the presence of crown-ether molecules was characterized by a Si/Al ratio of 2.7 (samples FauEmt-2a and FauEmt-4a). This value is in good agreement with the Si/Al ratio of FAU crystallized homogeneously from such gels in the absence of support crystals.[21] In the absence of crown-ether molecules, a value of 2.3 was obtained (sample FauEmt-1a). This Si/Al ratio is in the expected range for NaY zeolites synthesized from such inorganic gels. The series of samples with different degree of overgrowth formation (samples FauEmt-2c to FauEmt-2a, Table 6) displayed $Si/Al_{FAUlayer}$ ratios from 2.5 for FAU crystallites growing only at the corners and edges of the support crystals (sample FauEmt-2c), to 2.7 for a continuous film of FAU crystallites (sample FauEmt-2a).

In the sample FauEmt-2a, the EMT support crystals were completely covered by FAU crystallites. Therefore, the Si/Al ratio of the FAU layer could also be determined by X-ray photoelectron spectroscopy. The Si/Al ratio according to XPS, and representative of the external surface of the FAU crystallites was 2.8. The agreement with the NMR spectroscopic data which showed a Si/Al ratio of 2.7 was excellent. This provides a strong argument for the validity of the assumptions made in the exploitation of the NMR spectroscopic data with Equation (2), in general, and of the assumed intactness of the EMT support crystals, in particular. According to XPS, the Na/Al stoichiometry was close to unity (Na/Al = 0.97), confirming that the charges originating from the incorporation of Al atoms in the framework were balanced by Na cations.

Table 6. Framework Si/Al ratios and percentage distribution of the different Si(*n*Al) environments as determined by ^{29}Si MAS NMR spectroscopy

Sample	FAU (wt-%)	Si(4Al)	Si(3Al)	Si(2Al)	Si(1Al)	Si(0Al)	Si/Al overgrowth	Si/Al FAU layer
Support	0−19	0	5	25	52	18	3.4	–
FauEmt-1a	74	2	9	34	43	12	2.7	2.4
FauEmt-2a	80	1	9	32	44	14	2.9	2.7
FauEmt-4a	76	1	8	31	47	13	2.9	2.7
FauEmt-2b	62	1	7	31	46	15	3.0	2.6
FauEmt-2c	51	0	7	28	49	16	3.1	2.5

richment of the sample with aluminum through the FAU phase. Indeed, aluminum enrichment is known to give rise to an expansion of the unit cell.

For the calculation of the Si/Al ratio of the FAU layer based on the ^{29}Si MAS NMR spectroscopic data, the following assumptions were made. It was assumed that a number of EMT support crystals added did not become covered with FAU crystallites, but dissolved completely. Furthermore, it was assumed that there was neither dissolution, nor alteration of the Si/Al ratio of the EMT support crystals, which became overgrown by FAU crystallites. An additional complication in the calculation was the presence of FAU in the EMT support. Part of the FAU impurity was present as a polytypical intergrowth with EMT, the rest as isolated crystals with octahedral shapes. It was assumed that the FAU impurity had the same Si/Al ratio as the EMT phase, and that it dissolved or became overgrown in the same proportion as the EMT support crystals. These assumptions led to the expression of Equation (2) for the Si/Al ratio of the FAU layer, in which $fraction_{support}$ and $fraction_{FAUlayer}$

It was possible to determine the Si/Al ratio of individual FAU crystallites of sample FauEmt-2a by using electron nanoprobe analysis (nano-EDAX). It was found that the FAU crystallites grown at the corners and edges of the EMT support crystals had a Si/Al ratio of 2.5, whereas the FAU crystallites grown in the center of the basal $\{0001\}_{EMT}$ planes had an Si/Al ratio of 2.8. There were many more crystallites at faces than at corners and edges, thus explaining why the overall Si/Al ratio of the FAU layer, deter-

mined by NMR spectroscopy and XPS, corresponded to that on the $\{0001\}_{EMT}$ planes. The FAU crystallites start growing at the corners and edges of the EMT support crystals and hence the first FAU crystallites formed are richer in aluminum than the crystallites formed at a later stage. In a sample in which overgrowth formation was limited to the corners and edges of the support by increasing the amount of support crystals added, the Si/Al ratio was indeed 2.5 (sample FauEmt-2c, Table 6). The increase in the Si/Al ratio of the FAU crystallites during the overgrowth process may be explained by the decrease in the pH during the crystallization of the faujasite type zeolite in the presence of crown ethers.[23] Depletion of aluminum in the synthesis gel might be another reason for this behavior.

The EMT support crystals were prepared in the presence of 18-crown-6 ether, whereas the synthesis gel for the FAU layer optionally contained crown-ether molecules. The incorporation of crown-ether molecules in the support crystals and some selected overgrowth materials was studied with thermogravimetric-differential thermal analysis (TG-DTA). Typical TGA/DTA profiles of the EMT support crystals and a representative FAU-on-EMT overgrowth material, recorded under He/O_2 are given in Figure 12. The weight-losses observed during heating can be attributed to the endothermic desorption of water, followed by a multiple-step exothermic decomposition of crown-ether molecules.[34] On the basis of this last weight-loss, the crown-ether content of the support crystals, as well as of some selected overgrowth materials were calculated and expressed as the number of crown-ether molecules per 192 T-atoms, representing 8 large cages in both the FAU and the EMT structure (Table 7). The number of crown-ether molecules in the EMT support crystals corresponded to approximately 9.5 molecules per 8 cages (Table 7). The presence of an excess of crown-ether molecules relative to the number of cages is in agreement with previous data.[21] Assuming that the crown-ether content of the support crystals did not change during the overgrowth process, the amount of crown-ether molecules per 192 T-atoms in the FAU layer ($CE_{FAUlayer}$) could be related to the crown-ether content of the overgrowth ($CE_{overgrowth}$) according to Equation (3).

$$CE_{FAUlayer} = [CE_{overgrowth} - CE_{support} \times fraction_{support}]/fraction_{FAUlayer} \quad (3)$$

These numbers are given in Table 7. The FAU crystallites synthesized in the presence of crown-ether molecules (samples FauEmt-2a to FauEmt-5a) contain approximately one crown-ether molecule per cage, or eight per 192 T-atoms. Even without intentional addition of crown-ether molecules to the FAU synthesis gel, the FAU layer occluded some crown-ether molecules (samples FauEmt-1a to FauEmt-1c, Table 7). Comparison of the amount of crown-ether molecules in the inorganic FAU layer with the amount liberated by partial dissolution of the EMT support crystals showed that the dissolution process alone could not account for all crown-ether molecules incorporated in the FAU layer. Additional crown-ether molecules could be provided by the mother liquor surrounding the support crystals, or as molecules that are physisorbed on the external surface of the support crystals. These phenomena were more pronounced when more support crystals were used, thus resulting in an enhanced incorporation of crown-ether molecules in the FAU layer (Table 7).

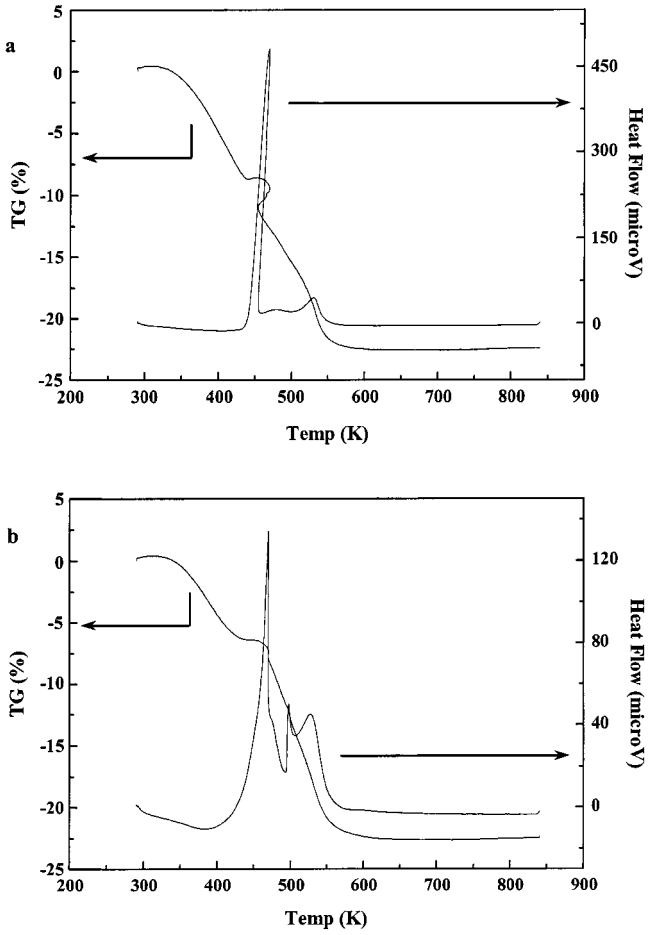

Figure 12. TGA/DTA profiles recorded under He/O_2 of (a) EMT support crystals and (b) sample FauEmt-2a; the oblique nature of the largest heat flow peak and the concomitant bump in the TG curve are due to the higher temperatures caused by the exothermic crown-ether decomposition[34]

Table 7. Crown-ether content of the support crystals, some FAU-on-EMT overgrowth materials and the FAU layer, as determined with TG-DTA

Sample	CE/192 T-atoms		
	support	overgrowth	FAU layer
FauEmt-2a	10.0	8.6	8.2
FauEmt-2b	10.0	8.9	7.9
FauEmt-2c	10.0	9.1	7.9
FauEmt-4a	9.1	8.3[a]–9.9[b]	8.0[a]–10.2[b]
FauEmt-5a	9.5	9.1[a]–10.9[b]	8.9[a]–11.4[b]
FauEmt-1a	9.8	4.9	2.6
FauEmt-1b	9.8	6.5	3.4
FauEmt-1c	9.8	7.9	3.8

[a] Assuming 18-crown-6 is exclusively present. – [b] Assuming 15-crown-5 is exclusively present.

Overgrowth Synthesis Efficiency

In this section, two aspects of synthesis efficiency are discussed, namely the FAU yield with respect to the gel and

the EMT losses due to partial dissolution of the support crystals. Comparison of the weight of EMT in the overgrowth product with the weight of EMT support crystals added, showed that part of the EMT phase dissolved (Table 2). In the calculations in the previous section, it was assumed that the FAU impurity phase of the EMT support crystals dissolved in the same proportion as the EMT phase. This assumption led to reasonable interpretations of the FAU and EMT contents of the FAU-on-EMT overgrowth materials and of the framework Si/Al ratios of the respective phases.

The assumed weights of FAU impurities dissolved during the overgrowth process are given in Table 2. The FAU yield with respect to the gel was obtained by subtracting the weight of the FAU impurity phase which did not dissolve from the weight of FAU in the final product, and dividing this value by the weight of synthesis gel (Table 2). In the experiments with three different FAU gel compositions (samples FauEmt-1a, FauEmt-2a and FauEmt-4a), the amount of FAU crystallites formed per gram of gel was about the same. Approximately 0.14 g (calcined amount) of the FAU structure type crystallized per gram of synthesis gel (Table 2). This value corresponds to a yield of ca. 55 wt-%, in terms of silicon, whereas the yield in terms of aluminum is approximately 100 wt-%, thus suggesting that the maximal possible conversion of the FAU gel was achieved. However, comparison of the EMT yield in the overgrowth product with the weight of EMT support crystals added (Table 2), showed that 24−47% of the support crystals did dissolve. The dissolution was most pronounced in hydrogels containing crown-ether with an OH^-/SiO_2 ratio of 0.75 (samples FauEmt-2a and FauEmt-4a, Table 2). Dissolution of a number of the support crystals enriched the synthesis gel with silicon and aluminum. Assuming that the aluminosilicate species generated through dissolution were consumed during the growth of the FAU phase, the yields of the FAU layer in terms of silicon and aluminum could be recalculated as ca. 45 and 80 wt-%, respectively. Aluminum remains the limiting factor with respect to the yields, as generally encountered with Y type zeolites.

Variation of the crystallization time between 1 and 5 d (samples FauEmt-2k to FauEmt-2o) only had a small effect on the amount of FAU formed per gram of FAU synthesis gel. On the other hand, the amount of support crystals dissolved during the overgrowth process remained constant until a crystallization time of 3 d, after which it increased substantially (Table 2). This observation provides additional evidence for the assumed intactness of the EMT core of the FAU-on-EMT overgrowth materials obtained in the three-day synthetic experiments. As long as there is gel and the overgrowth process is taking place, the EMT support crystals which are covered with FAU crystallites do not dissolve. When the overgrowth process is terminated, the mother liquor becomes depleted and the most siliceous part of the overgrowth, i.e. the EMT core, starts to dissolve. Synthesis time is, therefore, a critical synthesis parameter. Prolongation of the crystallization time might be used for the preparation of hollow particles with a shell composed of Al-rich FAU crystallites, by dissolving the Si-rich EMT core. Hollow crystals are expected to have favorable mass- and heat-transfer properties, and may be advantageous, for example, in rapid-pressure-swing adsorptive separations.

Quantification of the FAU-on-EMT overgrowth materials obtained using different amounts of support crystals (samples FauEmt-1a to FauEmt-1c and FauEmt-2a to FauEmt-2c) showed that the yield of FAU formed per gram of FAU synthesis gel decreased with an increasing amount of EMT crystals added, especially in presence of 18-crown-6 ether molecules (Table 2). A possible explanation for this decrease is that, although the percentage of dissolved support crystals diminishes when more support crystals are used, the absolute amount of support crystals dissolved per gram of FAU synthesis gel increases, thus perturbing the original optimized FAU gel composition to a larger extent.

Conclusions

In this paper, the potential of the two-step synthetic procedure for synthesizing systematic FAU-on-EMT overgrowth materials has been investigated. Inoculation of a FAU synthesis gel with a high sodium content (Na_2O/SiO_2 = 0.34 or 0.375) and which optionally contained crown-ether molecules, with EMT support crystals, resulted in the formation of a continuous film of FAU crystallites on the original micrometer-sized hexagonal-platelet EMT support crystals. The overgrowth was achieved at 373 K within 1 d. On the other hand, no crystallization took place from an FAU synthesis gel containing 15-crown-5 ether and with a low sodium content (Na_2O/SiO_2 = 0.24), unless this gel was aged for 3 d at room temperature prior to the addition of EMT support crystals. However, in this case the support crystals were not completely covered with FAU crystallites and a new population of isolated FAU crystals with octahedral morphology was obtained. Washing or washing, drying and calcining the support crystals before they were added to the FAU synthesis gel was detrimental and resulted in the formation of an undesirable population of isolated FAU crystals. Variation of the amount of support crystals added or the synthesis time showed that the FAU crystallites preferentially nucleate and grow on the corners and edges of the EMT support crystals. Only when the amount of the synthesized EMT support crystals per gram of synthesis gel is approximately 0.20 g, do the support crystals become completely coated with FAU crystallites.

The FAU-on-EMT overgrowth materials obtained were characterized in detail using a variety of physico-chemical characterization techniques. Quantification of the overgrowth materials with XRD revealed that the yield of FAU with respect to the gel was similar for the three types of gel compositions used. After 3 d at 373 K, the overgrowth process was complete and the supply of nutrients from the gel exhausted. The yield of FAU layer in terms of the gel decreased with an increasing amount of support crystals added. Of the EMT support crystals added, a fraction dis-

solved completely, whereas the rest became overgrown. The overgrown support crystals were not damaged and maintained their Si/Al ratio and their original micropore volume.

The dissolution behavior of the synthesized EMT crystals in basic solutions was investigated. The dissolution was found to cause the formation of pits over the entire surface. Extensive dissolution resulted in the formation of particles, which were more strongly dissolved at the center than at the outer rim. The EMT crystals dissolved in a block-wise manner and finally were decomposed into smaller fragments with Si/Al ratios as low as 1.3. Such debris from EMT dissolution were not observed in the overgrowth formation experiments.

The Si/Al ratio of the FAU crystallites was found to be dependent on the gel composition and on the position of the crystallites with respect to the surface of the EMT support. The first crystallites formed, which were positioned at the corners and edges of the EMT support crystals, were richer in aluminum than the crystallites formed at a later stage and present in the center of the basal $\{0001\}_{EMT}$ planes. FAU-on-EMT overgrowth materials synthesized in the presence of crown-ether molecules contain approximately one crown-ether per cage. Even in the absence of crown-ether molecules during the second synthetic step, the FAU phase occluded some crown-ether molecules, which were introduced with the synthesized EMT support crystals. This amount was more pronounced when more EMT support crystals were added to the inorganic FAU synthesis gel. Nitrogen physisorption measurements indicated that all pores were accessible to nitrogen. The low external surface areas of the FAU-on-EMT overgrowth materials were in agreement with the absence of mesopores and a tight fitting of the support and the overgrowing layer.

Experimental Section

Two-Step Synthesis: Hydrogels for the synthesis of FAU type zeolites were obtained following the procedure described by Feijen et al.,[21] and using Ludox HS-40 (DuPont), NaOH pellets (Merck), gibbsite (Fluka), 15-crown-5 ether (1,4,7,10,13-pentaoxacyclopentadecane, Acros) or 18-crown-6 ether (1,4,7,10,13,16-hexaoxacyclooctadecane, Acros) and distilled water. A given amount of the synthesized EMT support crystals was added to these gels, which were optionally aged for 3 d at room temperature. The resulting mixtures were stirred for 15 min and subsequently transferred into PTFE-lined stainless-steel autoclaves. These autoclaves were heated to the crystallization temperature of 373 K under quiescent conditions without aging. After the crystallization time had elapsed, the solid products were recovered by vacuum filtration, washed with deionised water until the pH value of the wash water was below 10 and dried at 333 K. Calcination was done in a muffle furnace at 823 K for 20 h. − EMT support crystals were prepared in a similar way to the hydrogels with the following molar oxide ratios: 10 SiO_2/1 Al_2O_3/2.4 Na_2O/0.97 18-crown-6/135 H_2O. − These gels were aged in PTFE-lined stainless-steel autoclaves for 3 d at room temperature and subsequently heated to the crystallization temperature of 373 K at autogenous pressure without stirring. After 11 d, the autoclaves were cooled in water and a wet cake of the EMT support crystals was recovered by vacuum filtration.

Powder X-ray Diffraction (XRD): XRD patterns were collected with an automated Siemens D-5000matic diffractometer using Cu-K_α radiation. XRD profiles were recorded in the range of 2θ values between 4 and 55°, with steps of 0.02° and counting times of 1.2 s.

Scanning Electron Microscopy (SEM): SEM pictures were taken with a Jeol superprobe 733 and of a Philips XL30 FEG apparatus. A gold film was sputtered onto the samples supported on alumina disks prior to their observation.

High-Resolution Transmission Electron Microscopy (HRTEM): HRTEM investigations were carried out with a 200-kV Philips CM200 Ultra Twin apparatus with a point-to-point resolution of 0.19 nm. The zeolite powder was deposited onto a carbon support and remained stable under the electron beam irradiation for at least several minutes. Nano-EDAX (energy-dispersive analysis of X-rays) was performed with the same apparatus equipped with a Noran EDX-detector having an ultra-thin window. The TEM was operated in the nanoprobe-mode, which implies that the electron beam diameter was reduced to 5 nm or even smaller.

NMR Spectroscopy: ^{29}Si magic angle spinning (MAS) NMR spectroscopy was performed with a Bruker MSL400 (9.4 T) spectrometer at 79.5 MHz, with a pulse length of 4 μs, a repetition time of 5 s, a spinning rate of 4 kHz and 11 000 scans. The ^{29}Si chemical shifts were reported relative to Me_4Si.

X-ray Photoelectron Spectroscopy (XPS): XPS was carried out with a Perkin−Elmer PHI 5500 ESCA system using monochromatic Al-K_α radiation. The binding energies were referred to C(1s) = 286.4 eV. The evaluation of the surface composition was performed using the intensities of the Na(1s), O(1s), Si(2p), and Al(2p) lines.

Nitrogen Physisorption: Nitrogen physisorption isotherms at 77 K were recorded with an Omnisorp-100 analyzer from Coulter, operating in the continuous flow mode. Before recording the isotherms, calcined samples were outgassed at 673 K under high vacuum (10^{-6} kPa) for at least 12 h. Micropore volumes and specific external surface areas were derived from the isotherms using the t-plot method of Lippens and de Boer.[35] The Horvath−Kawazoe method[36] was applied to determine the micropore diameter.

Thermogravimetric and Differential Thermal Analysis (TG-DTA): TG-DT analyses were performed simultaneously with a Setaram TGA92 thermobalance under oxygen/helium (25:75 vol-%) using typically 30 mg of sample and a flow of 35 mL/min. The temperature was increased at a rate of 5 K/min from room temperature to 823 K.

Acknowledgments

A. M. G. and P. J. G. acknowledge the Flemish IWT for a Ph. D. grant and the Flemish FWO for a position as Research Director, respectively. The authors are grateful to F. Pelgrims for the technical assistance with the SEM. The work was sponsored by the Belgian Federal Government in the frame of the IUAP-PAI program.

[1] C. N. R. Rao, J. M. Thomas, *Acc. Chem. Res.* **1985**, *18*, 113−119.
[2] M. W. Anderson, K. S. Pachis, F. Prébin, S. W. Carr, O. Terasaki, T. Ohsuna, V. Alfreddson, *J. Chem. Soc., Chem. Commun.* **1991**, 1660−1664.
[3] M. M. J. Treacy, D. E. W. Vaughan, K. G. Strohmaier, J. M. Newsam, *Proc. R. Soc. Lond. A* **1996**, *452*, 813−840.
[4] K. P. Lillerud, J. H. Raeder, *Zeolites* **1986**, *6*, 474−483.
[5] P. A. Jacobs, J. A. Martens, "Synthesis of High-Silica Alumino-

silicate Zeolites", *Stud. Surf. Sci. Catal.*, vol. 33, Elsevier Science B. V., Amsterdam, **1987**.
[6] J. M. Thomas, G. R. Millward, *J. Chem. Soc., Chem. Commun.* **1982**, 1380−1383.
[7] G. R. Millward, S. Ramdas, J. M. Thomas, M. T. Barlow, *J. Chem. Soc., Faraday Trans. 2* **1983**, *79*, 1075−1082.
[8] M. E. Leonowicz, D. E. W. Vaughan, *Nature* **1987**, *329*, 819−821.
[9] D. E. W. Vaughan, K. G. Strohmaier, in: *Zeolite Synthesis* (Eds.: M. L. Occelli, H. E. Robson), ACS Symp. Ser. No. 398, Washington, DC, **1989**, p. 506.
[10] G. R. Millward, S. Ramdas, J. M. Thomas, *Proc. R. Soc. Lond. A* **1985**, *399*, 57−71.
[11] R. Szostak, K. P. Lillerud, in: "Zeolites and Related Microporous Materials: State of the Art 1994" (Eds.: J. Weitkamp, H. G. Karge, H. Pfeifer, W. Hölderich), *Stud. Surf. Sci. Catal.*, vol. 84, Elsevier Science B. V., Amsterdam, **1994**, p. 535.
[12] W. S. Wise, R. W. Tschernich, *Am. Mineral.* **1976**, *61*, 853−858.
[13] W. S. Wise, D. Pierce, *Scanning Electron Microsc.* **1981**, 633−636.
[14] E. de Vos Burchart, J. C. Jansen, H. van Bekkum, *Zeolites* **1989**, *9*, 432−435.
[15] D. W. Breck, *Zeolite Molecular Sieves: Structure, Chemistry and Use*, John Wiley, New York, **1974**.
[16] A. D. Randolph, M. A. Larson, *Theory of Particulate Processes: Analysis and Techniques of Continuous Crystallization*, Academic Press, New York, **1971**.
[17] L. D. Rollmann, U. S. Patent 4,148,713 **1979**.
[18] S. J. Miller, U. S. Patent 4,394,251 **1983**; US Patent 4,394,362 **1983**.
[19] W. T. Koetsier, Eur. Patent 55,044 **1984**.
[20] A. M. Goossens, B. H. Wouters, V. Buschmann, J. A. Martens, *Adv. Mater.* **1999**, *11*, 561−564.
[21] E. J. P. Feijen, K. De Vadder, M. H. Bosschaerts, J. L. Lievens, J. A. Martens, P. J. Grobet, P. A. Jacobs, *J. Am. Chem. Soc.* **1994**, *116*, 2950−2957.
[22] A. J. Bons, J. L. Lievens, J. P. Verduijn, W. J. Mortier, *Microsc. Res. Technol.* **1993**, *25*, 175−176.
[23] F. Delprato, L. Delmotte, J. L. Guth, L. Huve, *Zeolites* **1990**, *10*, 546−552.
[24] L.-Y. Hou, R. W. Thompson, *Zeolites* **1989**, *9*, 526−530.
[25] E. A. Tsokanis, R. W. Thompson, *Zeolites* **1992**, *12*, 369−373.
[26] V. Buschmann, A. L. Yonkeu, G. Miehe, H. Fuess, A. M. Goossens, J. A. Martens, manuscript in preparation.
[27] R. K. Iler, *The Chemistry of Silica*, John Wiley, New York, **1979**.
[28] R. M. Dessau, E. W. Valyocsik, N. H. Goeke, *Zeolites* **1992**, *12*, 776−779.
[29] A. Cizmek, B. Subotic, I. Smit, A. Tonejc, R. Aiello, F. Crea, A. Nastro, *Microporous Mater.* **1997**, *8*, 159−169.
[30] R. M. Barrer, *Hydrothermal Chemistry of Zeolites*, Academic Press, London, **1982**.
[31] A. Katovic, B. Subotic, I. Smit, Lj. A. Despotovic, M. Curic, in: *Zeolite Synthesis* (Eds.: M. L. Occelli, H. E. Robson), ACS Symp. Ser. No. 398, Washington, DC, **1989**, p. 124.
[32] E. J. P. Feijen, J. L. Lievens, J. A. Martens, P. J. Grobet, P. A. Jacobs, *J. Phys. Chem.* **1996**, *100*, 4970−4975.
[33] J. Klinowski, in: *Stud. Surf. Sci. and Catal.*, vol. 52, Elsevier Science B. V., Amsterdam, **1989**, p. 39.
[34] E. J. P. Feijen, J. A. Martens, P. A. Jacobs, *J. Chem. Soc., Faraday Trans.* **1996**, *92*, 3281−3285.
[35] B. C. Lippens, J. H. de Boer, *J. Catal.* **1965**, *4*, 319−323.
[36] G. Horvath, K. Kawazoe, *J. Chem. Eng. Jpn.* **1983**, *16*, 470−473.

Received October 4, 2000
[I00373]